JOURNAL OF GEOPHYSICAL RESEARCH, VOL. 101, NO. B5, PAGES 11,695–11,699, MAY 10, 1996

Analysis of fractures intersecting Kahi Puka Well 1 and its relation to the growth of the island of Hawaii

Roger H. Morin and Frederick L. Paillet
U.S. Geological Survey, Denver, Colorado

Abstract. As part of the Hawaii Scientific Drilling Project, Kahi Puka Well 1 penetrated about 275 m of Mauna Loa basalts overlying a sequence of Mauna Kea flow units as it was drilled and cored to a total depth of 1053 m below land surface. A borehole televiewer (BHTV) was run in most of the well in successive stages prior to casing in order to obtain magnetically oriented acoustic images of the borehole wall. A total of 283 individual fractures were identified from this log and characterized in terms of strike and dip. These data are divided into three vertical sections based upon age and volcanic source, and lower hemisphere stereographic plots identify two predominant, subparallel fracture subsets common to each section. Assuming that most of the steeply dipping fractures observed in the BHTV log are tensile features generated within basalt flows during deposition and cooling, this fracture information can be combined with models of the evolution of the island of Hawaii to investigate the depositional history of these Mauna Loa and Mauna Kea basalts over the past 400 kyr. The directions of high-angle fractures appear to be generally parallel to topography or to the coastline at the time of deposition, as is supported by surface mapping of modern flows. Consequently, an overall counterclockwise rotation of about 75° in the strike of these fractures from the bottom to the top of the well represents a systematic change in depositional slope direction over time. We attribute the observed rotation in the orientations of the two predominant fracture subsets over the past 400 kyr to changes in the configurations of volcanic sources during shield building and to the structural interference of adjacent volcanoes that produces shifts in topographic patterns.

Introduction

The island of Hawaii is composed of five melded volcanoes: Kohala, Hualalai, Mauna Kea, Mauna Loa, and Kilauea (Figure 1). Of these, Mauna Kea is the highest, and Mauna Loa is the largest by volume. Figure 1 also shows the major rift and fault zones located on present-day Hawaii, along with the location of Kahi Puka Well 1 (KP-1). KP-1 was drilled and cored as part of the Hawaii Scientific Drilling Project (HSDP) in order to obtain a nearly continuous record of the output of an oceanic volcano over a substantial interval of its shield-building phase of activity. Background information regarding this project and a summary of preliminary results are presented by *Stolper et al.* [this issue].

KP-1 penetrated a sequence of basalt flows and thin sedimentary interbeds [*Hawaii Scientific Drilling Project (HSDP)*, 1994] and reached a total depth of 1053 m below land surface (mbls). A series of geophysical logs was obtained in this well to complement core data and to provide vertically continuous profiles of various formation properties. As part of this scientific logging program, a borehole televiewer (BHTV) was run through most of the well in successive stages prior to setting of casing. The BHTV provides magnetically oriented acoustic images of the borehole wall from which certain rock characteristics may be visually investigated [*Zemanek et al.*, 1970]. Televiewer logs obtained in this well extend from just below initial surface casing (65 mbls) down close to total depth (1045 mbls). Regretably, one section from 560 to 710 m could not be logged due to unstable hole conditions, and this interval is not included in this analysis.

Paper number 95JB03848.

The data were digitized in terms of both acoustic amplitude and travel time according to *Barton* [1988] and as demonstrated by *Barton and Zoback* [1992]. These processed logs have been integrated into several complementary studies that investigate the lithostratigraphic and hydrogeologic characteristics of this site [*Paillet and Thomas*, this issue; *Thomas et al.*, this issue]. In this paper we focus on the detailed analysis of fractures that intersect the well as identified in the BHTV images and interpret the results in terms of the growth and evolution of the island of Hawaii.

Fracture Data

An example of an acoustic borehole image generated from the televiewer is depicted in Figure 2 across the depth interval from 1020 to 1024 mbls. This 4-m-thick interval encompasses a thin, sedimentary interbed bounded above and below by thick aphyric-basalt units [*HSDP*, 1994]. The densely fractured section represents a weathered zone intersected by a thin, subhorizontal layer of soil; the more competent sections represent basalt flows, each of which is intersected by an overt, steeply dipping fracture. Because the log is magnetically oriented, the strike and dip of these isolated fractures can be computed by means of a simple geometric exercise after correction for local magnetic declination [e.g., *Paillet*, 1993; *Barton and Zoback*, 1992].

A total of 283 fractures intersecting this borehole were reliably described in terms of strike and dip. Numerous intervals

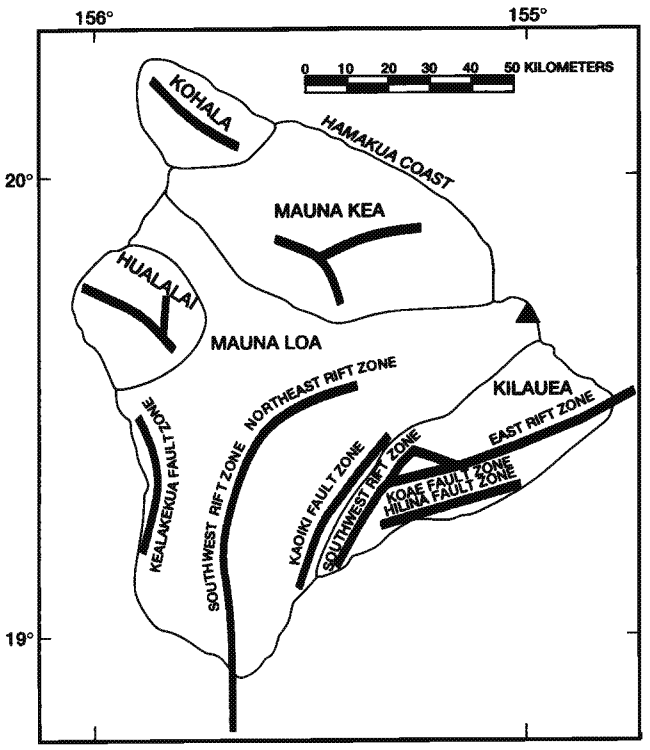

Figure 1. Island of Hawaii showing the five volcanoes and their boundaries, major rift zones, and fault zones [after *Peterson and Moore*, 1987]. Triangle indicates location of KP-1.

were highly damaged, altered, or washed out, and few unique fractures could be distinguished from the complex background structure. However, as illustrated in Figure 2, other sections consisted of denser, intact basalt flows where individual fractures were more obvious. Therefore an inherent sampling bias probably exists in these data toward more competent rock and away from rubbly and weathered deposits.

These fracture data are divided into three vertical sections based upon age and volcanic source; all ages referred to in this paper are based upon $^{40}Ar/^{39}Ar$ and K/Ar dating results obtained on core samples and reported by *Sharp et al.* [this issue]. (1) The upper section ranges from 65 mbls to the contact separating the surficial Mauna Loa basalts from the underlying Mauna Kea basalts, identified to be at a depth of about 275 mbls [*Thomas et al.*, this issue]. This section represents approximately the youngest 180 ka of depositional activity. (2) The intermediate section consists entirely of Mauna Kea subaerial lavas and extends from this contact down to the zone of missing data (275–560 mbls). Ages encompassed by this vertical section range from about 180 to 340 ka. (3) The lower section continues from the bottom of this data gap to approach total depth (710–1045 mbls). Mauna Kea basalts again compose this interval, with ages extending from approximately 360 to 400 ka. Analysis of the televiewer data from the perspective of this vertical record enables us to examine particular fracture characteristics as they evolve over time.

Cumulative information regarding fracture strike and dip corresponding to each designated section is plotted in Figure 3 in the form of equal-area, lower hemisphere stereographic projections. This type of diagram is a representation of pole-to-plane fracture densities converted to shaded contours using spherical Gaussian statistics [*Kamb*, 1959]. Values listed for the contour intervals (CI) indicate particular increments of the standard deviation σ and were chosen to optimize visual recognition. Each of the diagrams in Figure 3 depicts two high-density zones which delineate predominant fracture subsets within the general fracture population.

A total of 69 separate fractures were identified in the upper 275 m of the well (Figure 3a), and two subsets of nearly parallel, high-angle fractures clearly emerge from the overall population. These represent fracture planes oriented at about N30°W. Another 70 fractures were identified from the intermediate section, and the stereographic plot shown in Figure 3b indicates that the two major subsets remain, although their orientations have been rotated clockwise about 45° and now strike at approximately N15°E. In the lower section, 144 additional fractures were identified. The presence of the two predominant fracture subsets persists to total depth and their orientations are now essentially parallel at about N45°E (Figure 3c). This represents a further clockwise rotation of 30° compared to the section above and a counterclockwise rotation in a chronological sense of approximately 75° over the past 400 kyr.

Interpretation

The major rift zones on the island of Hawaii are shown in Figure 1. These are usually a surficial expression of extensional features and are commonly coincident with topographic ridges.

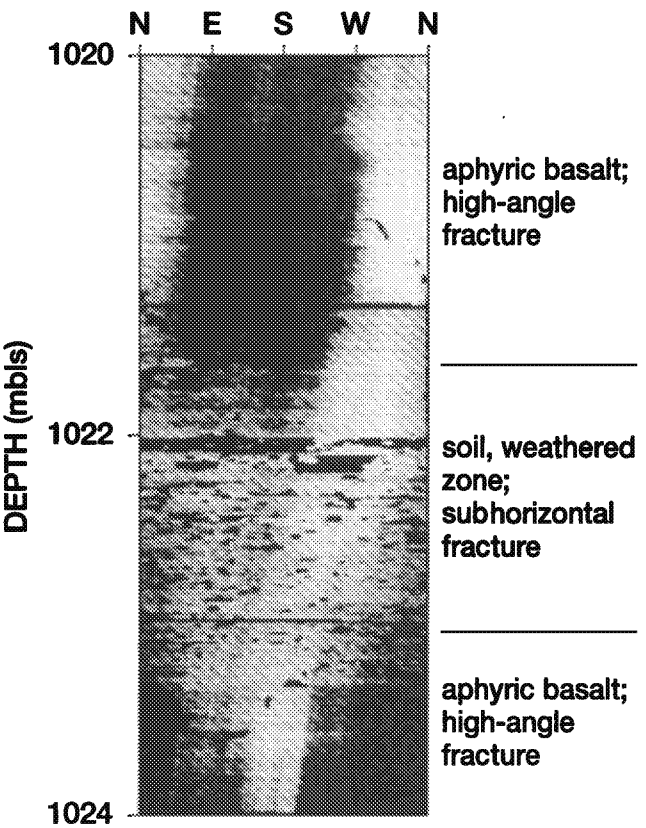

Figure 2. Example of televiewer image processed in terms of acoustic amplitude across depth interval from 1020 to 1024 m below land surface (mbls). High-angle fractures intersecting basalt units dip approximately to the east (low point of sinusoids) at about 75° to 80°. Core descriptions reported from *Hawaii Scientific Drilling Project* [1994].

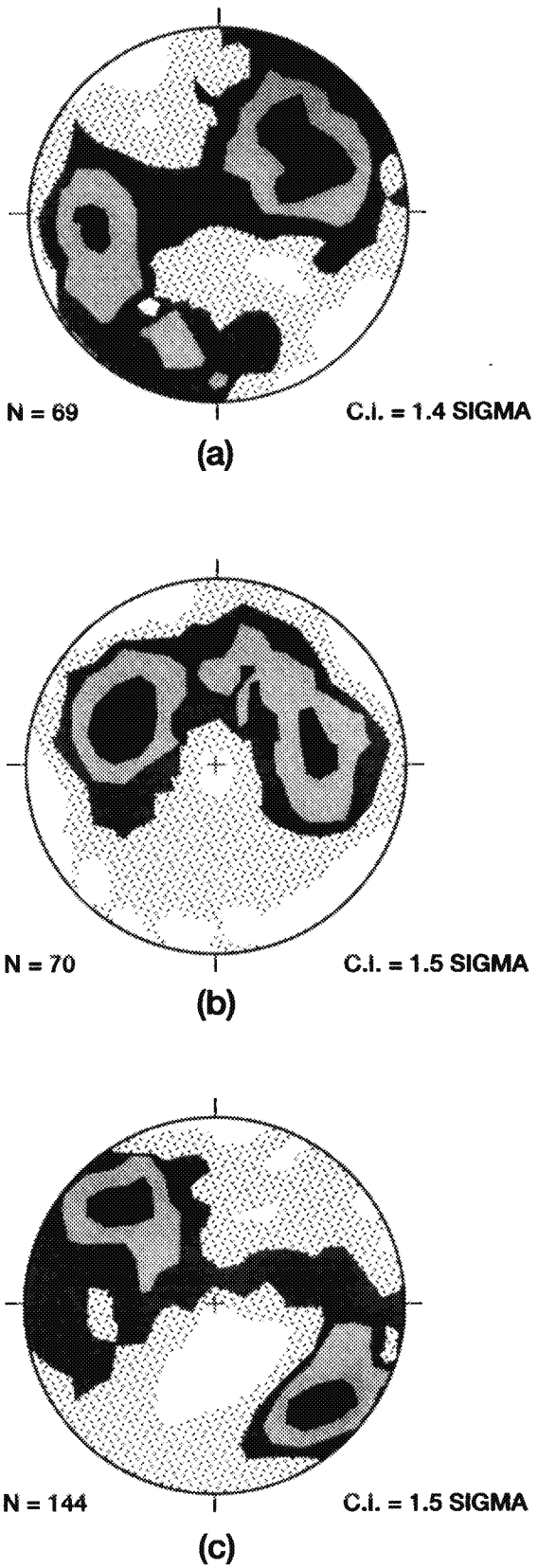

Figure 3. Stereographic projections of fracture strike-and-dip data associated with the three depth intervals. (a) upper, depth from 65 to 275 mbls; age from 0 to 180 ka; (b) intermediate, depth from 275 to 560 mbls; age from 180 to 340 ka; (c) lower, depth from 710 to 1045 mbls; age from 360 to 400 ka.

This generalized structure also extends below sea level with the development of submarine rift zones [*Fornari*, 1987]. The relative locations of individual rift zones with respect to their volcanic centers have been examined by *Fiske and Jackson* [1972] and by *Lipman* [1980], among others. These investigators conclude that the particular locations of shallow-level rift zones are primarily controlled by the gravitational stresses produced within a shield and, to a lesser extent, by the positions of preexisting shields that buttress the nascent volcanoes. These types of forces are presently contributing to the displacement of Kilauea [*Hill and Zucca*, 1987; *Tilling and Dvorak*, 1993]. In addition, *Mattox* [1993] describes the physical characteristics of modern Kilauea flows and the development of large cracks parallel to the coastline associated with lava bench collapse.

We apply these observations to this analysis of fractures intersecting KP-1 and assume that the initiation and propagation of fractures within individual basalt units are generated by the surficial stress field acting at the time of deposition. This implies that many of the fractures identified in the BHTV log formed in tension during shield-building activity as a result of an extensional stress regime controlled by topography and the relative location of adjacent structures. *Pollard and Aydin* [1988] state that fractures often form initially in tension and that joints produced by the cooling of a lava flow usually are perpendicular to the flow surface. The vertical extent of these joint patterns is limited by the thickness of the basalt unit and, as seen in Figure 2, may be constrained by the presence of a sedimentary interbed.

The fracture information collected in this well based on the BHTV logs enables us to separate the high-angle and presumably tensile fractures from the general fracture population in order to examine the development of these extensional features as a function of depth and its surrogate, age. Only fractures with dips greater than 50° are considered from the three stereographic plots shown in Figure 3, and their orientations are presented as rose diagrams in Figure 4 alongside a conceptual model for the evolution and growth of the island of Hawaii as proposed by *Moore and Clague* [1992]. The location of the drill site (triangle) is projected to earlier time on the present-day base map. Since all lavas recovered from KP-1 are subaerial, it appears that the drill site was above sea level considerably earlier in the evolution of the island than is postulated by *Moore and Clague* [1992]. These investigators based their model on a 500-kyr volcanic life cycle. However, new information obtained from this drilling project indicates that this estimate is too short by a factor of ~2; the life span of a volcano on the island of Hawaii is closer to 1 Myr [*DePaolo and Stolper*, this issue]. Thus the 200 ka and 100 ka ages listed in Figure 4 should be roughly 400 ka and 200 ka, respectively, and the rose diagrams corresponding to these revised ages are presented alongside the appropriate panel.

Each rose diagram is associated with a particular time interval and, correspondingly, with a particular stage of island growth; all three diagrams depict fracture orientations that are generally parallel to topography or the coastline at the time of deposition. At early time (400–360 ka), Mauna Kea is the source volcano and the two predominant fracture subsets are parallel to each other. At later time (340–180 ka), Mauna Kea is waning and its structural interaction with Mauna Loa produces a change in slope direction at the projected drill site. This activity appears to have two effects on the fracture population: (1) there is a slight counterclockwise rotation in the

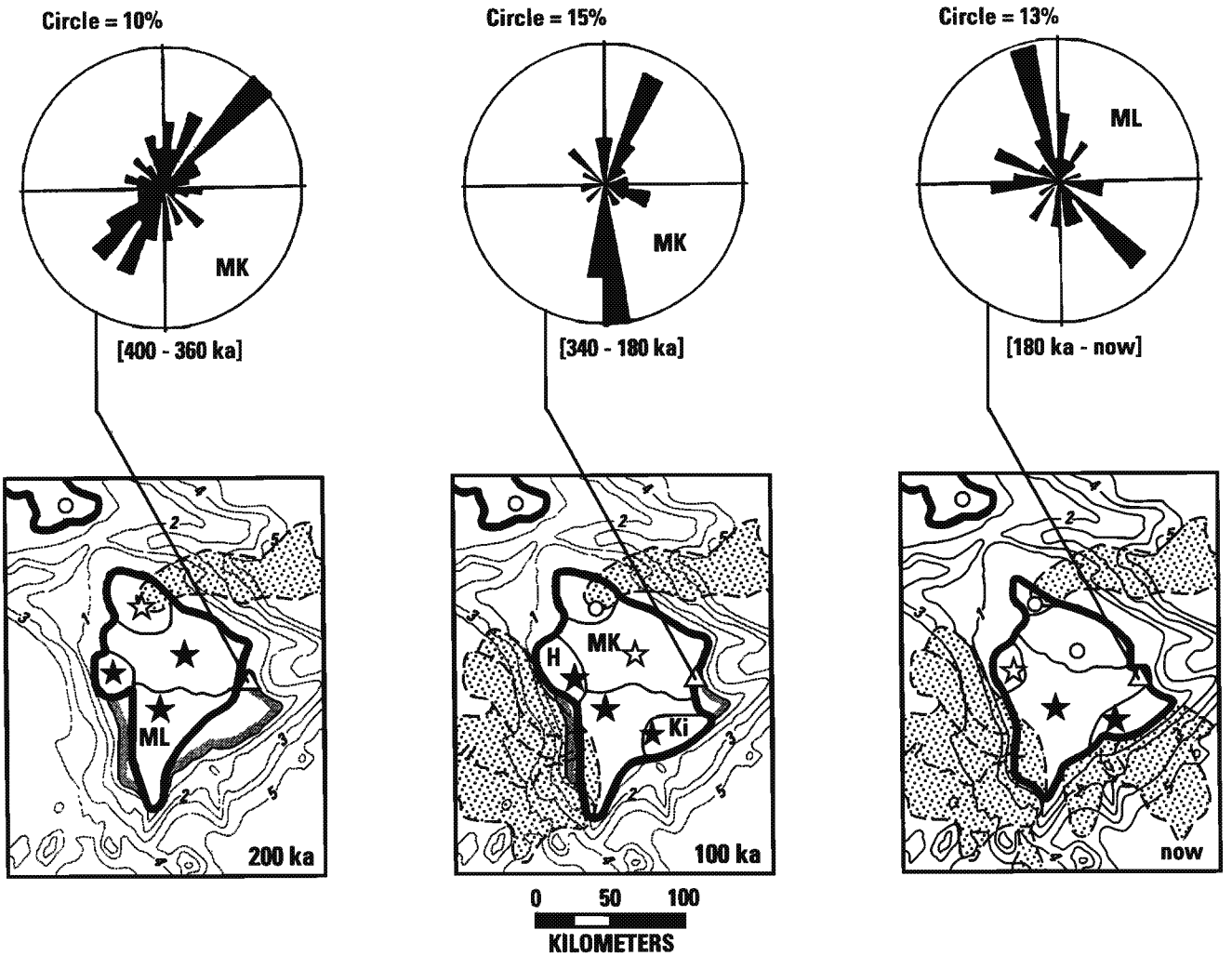

Figure 4. Evolution and growth of island of Hawaii on present-day base map [from *Moore and Clague*, 1992], with corresponding fracture orientation data associated with each stage. H refers to Hualalai, MK to Mauna Kea, ML to Mauna Loa, and Ki to Kilauea. Bathymetric contours show depth in kilometers, and landslides are depicted by stippled pattern. Solid stars represent vigorous subaerial volcanic centers, open stars represent waning subaerial volcanic centers, and open circles represent dormant or near-dormant subaerial volcanic centers. The location of the drill site is projected to earlier time and identified by a triangle. Rose diagrams depict strike direction (for fractures with dips >50° only) corresponding to ranges in age assigned to the three sections of the well from core analyses. Ages of the three stages taken from *Moore and Clague* [1992] are too young by a factor of ~2 (see text).

general fracture population, and (2) the two major fracture subsets are no longer parallel. These characteristics are also evident in the late fracture data (180 ka to present). Counterclockwise rotation continues, and the orientations of the fracture subsets seem to reflect the influences of both the Mauna Loa and Kilauea volcanic centers. *Stearns and Clark* [1930] report that the growth of Kilauea against the southeast flank of Mauna Loa produced a change in the behavior pattern of the Mauna Loa fault systems. It also produced shifts in slope direction and depositional patterns, as is evident in the two primary fracture modes depicted by the rose diagram.

Discussion

Ages of core samples reported by *Sharp et al.* [this issue] and a model for island evolution proposed by *Moore and Clague* [1992] provide an interpretive framework from which to examine the depositional environments of Mauna Loa and Mauna Kea basalts penetrated by KP-1. We assume that most of the steeply dipping fractures identified in the televiewer images are tensile fractures generated within basalt units during deposition and cooling and proceed to analyze statistically the distributions of these fractures.

Two predominant fracture subsets are identified, and their systematic rotation as a function of depth and age, as shown in Figure 3, represents a methodical change in depositional slope direction over the past 400 kyr. The clear emergence of these subsets common to all three depth intervals indicates that postdepositional forces have not dramatically altered fracture patterns. A certain degree of structural stability may be inferred from the lack of major landslides in this area (Figure 4).

An overall counterclockwise rotation of about 75° has occurred in the direction of high-angle fractures, from an early NE-SW orientation to the present-day NW-SE direction. Since fracture orientations appear to be generally parallel to topog-

raphy or the coastline at the time of deposition, we attribute this rotation to changes in location of volcanic sources and the relative structural impact of adjacent volcanoes on topography. In this instance, the chronological record of fracture orientation can be analyzed in terms of stress history and the reconstruction of island growth at a particular location.

Acknowledgments. We are grateful to D. Moos, B. Haimson, and K. Kim for providing thorough and thoughtful reviews which improved this manuscript significantly. Additional discussions with R. Denlinger were very helpful. We also thank R. Almendinger for his generous distribution of the software package STEREONET.

References

Barton, C. A., In-situ stress measurement techniques for deep drillholes, Ph.D. thesis, Stanford Univ., Stanford, Calif., 1988.

Barton, C. A., and M. D. Zoback, Self-similar distribution and properties of macroscopic fractures at depth in crystalline rock in the Cajon Pass Scientific Drill Hole, *J. Geophys. Res.*, *97*, 5181–5200, 1992.

DePaolo, D. J., and E. M. Stolper, Models of Hawaiian volcano growth and plume structure: Implications of results from the Hawaii Scientific Drilling Project, *J. Geophys. Res.*, this issue.

Fiske, R. S., and E. D. Jackson, Orientation and growth of Hawaiian volcanic rifts: The effect of regional structure and gravitational stresses, *Proc. R. Soc. London*, *329*, 299–326, 1972.

Fornari, D. J., The geomorphic and structural development of Hawaiian submarine rift zones, *U.S. Geol. Surv. Prof. Pap.*, *1350*, 125–132, 1987.

Hawaii Scientific Drilling Project (HSDP), *Core-Logs*, 471 pp., edited by E. Stolper and M. Baker, Calif. Inst. of Technol., Pasadena, 1994.

Hill, D. P., and J. J. Zucca, Geophysical constraints on the structure of Kilauea and Mauna Loa volcanoes and some implications for seismomagmatic processes, *U.S. Geol. Surv. Prof. Pap.*, *1350*, 903–917, 1987.

Kamb, W. B., Ice petrofabric observations from Blue Glacier, Washington, in relation to theory and experiment, *J. Geophys. Res.*, *64*, 1891–1910, 1959.

Lipman, P., The southwest rift zone of Mauna Loa: Implications for structural evolution of Hawaiian volcanoes, *Am. J. Sci.*, *280-A*, 752–776, 1980.

Mattox, T. N., Where lava meets the sea: Kilauea volcano, Hawaii, *Earthquakes Volcanoes*, *24*, 160–177, 1993.

Moore, J. G., and D. A. Clague, Volcano growth and evolution of the island of Hawaii, *Geol. Soc. Am. Bull.*, *104*, 1471–1484, 1992.

Paillet, F. L., Application of borehole geophysics in the characterization of flow in fractured rocks, *U.S. Geol. Surv. Water Res. Invest. Rep.*, *93-4214*, 36 pp., 1993.

Paillet, F. L., and D. M. Thomas, Hydrogeology of the Hawaii Scientific Drilling Project borehole KP-1, 1, Hydraulic conditions adjacent to the well bore, *J. Geophys. Res.*, this issue.

Peterson, D. W., and R. B. Moore, Geologic history and evolution of geologic concepts, island of Hawaii, *U.S. Geol. Surv. Prof. Pap.*, *1350*, 149–189, 1987.

Pollard, D. D., and A. Aydin, Progress in understanding jointing over the past century, *Geol. Soc. Am. Bull.*, *100*, 1181–1204, 1988.

Sharp, W. D., B. D. Turrin, P. R. Renne, and M. A. Lanphere, The $^{40}Ar/^{39}Ar$ and K/Ar dating of lavas from the Hilo 1-km core hole, Hawaii Scientific Drilling Project, *J. Geophys. Res.*, this issue.

Stearns, H. T., and W. O. Clark, Geology and water resources of the Kau District, Hawaii, *U.S. Geol. Surv. Water Supply Pap.*, *616*, 194 pp., 1930.

Stolper, E. M., D. J. DePaolo, and D. M. Thomas, Introduction to special section: Hawaii Scientific Drilling Project, *J. Geophys. Res.*, this issue.

Thomas, D. M., F. L. Paillet, and M. E. Conrad, Hydrogeology of the Hawaii Scientific Drilling Project borehole KP-1, 2, Groundwater geochemistry and regional flow patterns, *J. Geophys. Res.*, this issue.

Tilling, R. I., and J. J. Dvorak, Anatomy of a basaltic volcano, *Nature*, *363*, 125–133, 1993.

Zemanek, J., E. E. Glenn, L. J. Norton, and R. L. Caldwell, Formation evaluation by inspection with the borehole televiewer, *Geophysics*, *35*, 254–269, 1970.

R. H. Morin and F. L. Paillet, U.S. Geological Survey, MS 403, Denver Federal Center, P.O. Box 25046, Denver, CO 80225. (e-mail: rhmorin@borehole.cr.usgs.gov)

(Received April 24, 1995; revised December 14, 1995; accepted December 19, 1995.)